Strain-based design procedures for spiral-welded steel tubes in combined walls

Gresnigt, Nol; van Es, Sjors; Vasilikis, D; Karamanos, SA

Publication date
2016

Document Version
Accepted author manuscript

Published in
Proceedings of the International Colloquium on Stability and Ductility of Steel Structures

STRAIN-BASED DESIGN PROCEDURES FOR SPIRAL-WELDED STEEL TUBES IN COMBINED WALLS

Arnold M. Gresnigt[a], Sjors H.J. van Es[a], Daniel Vasilikis[b] and Spyros A. Karamanos[b]

[a] *Delft University of Technology, Delft, The Netherlands*
[b] *University of Thessaly, Volos, Greece*

Abstract: Spiral-welded steel tubes with diameter to wall thickness ratios between 60 and 140 are often employed in combined wall systems with local buckling as governing failure mode. The current design rules in Eurocode 3 (EN 1993-5 and EN 1993-1-6) are not capable to obtain a good estimate of the real strength and deformation capacity. In a European RFCS project called Combitube, the structural behaviour of spiral-welded steel tubes has been investigated. An analytical model has been developed that gives more economic designs with a better balanced safety level.

1. Introduction

Spiral-welded steel tubes are often employed in combined wall systems, e.g. for quay wall systems as indicated in Fig. 1. In these applications, the diameter to wall thickness ratio (D/t) ranges between 60 and 140. The main loading is bending in combination with normal force, earth loads and tensile or compressive loads from the infill sheeting. The governing failure mode is local buckling in the inelastic range of the steel.

The current design rules in Eurocode 3 (EN 1993-5 and EN 1993-1-6) follow a design approach based on stress resultants, rather than strains and deformations. It has been shown that these current design rules are not well suited for tubes in combined wall systems. They are not capable to obtain a good estimate of the real strength and deformation capacity and lead to uneconomic designs. Within the framework of a European RFCS project called Combitube, the structural behaviour of spiral-welded tubes for application in combined walls has been investigated. Full-scale four-point bending tests and extensive numerical parametric studies have been performed [1][7][8][9]. Based on the analytical formulation initially developed for buried pipelines [3][6] and the results of the Combitube research, an analytical model has been developed for tubes in combined walls including the effect of the following parameters:

- Diameter to wall thickness ratio (for tubes in CombiWalls usually between 60 and 140).
- Stress-strain properties of the steel, in particular the strain hardening properties.
- Presence of normal (axial) force and shear force in the tube.
- Transverse forces from infill sheeting.
- Cross-sectional ovalisation.
- Initial pipe wall short-wave wrinkling patterns in longitudinal direction.
- Other geometrical Imperfections: offset at girth welds ("high-low"), dimples.
- Residual stresses due to the manufacturing cold-bending process.

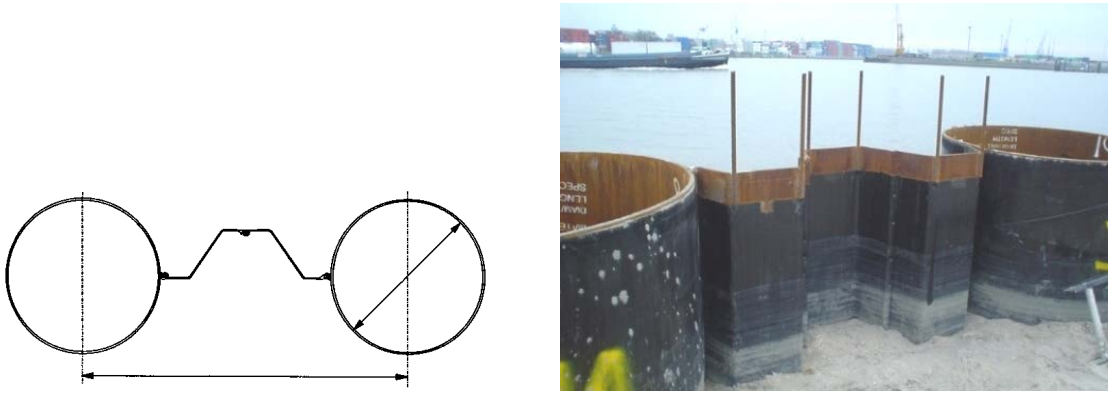

Fig. 1: Schematic and photo of a combined wall of tubes and infill sheeting, also called CombiWall; the infill sheeting is connected to the tubes with welded slots

2. Bending moment curvature diagram

First the bending moment curvature diagram is constructed in pure bending without the effect of other influences such as ovalisation, imperfections, residual stresses, etc. Thereafter the effect of other influences is considered. The equations are set up for thin walled tubes. This allows simplified equations for the cross-section quantities with sufficient accuracy for the present D/t range.

2.1 Moment curvature without other influences

A bilinear stress strain diagram is assumed (no strain hardening). For the elastic part it gives:

$$\begin{aligned} &M = \kappa \cdot EI \quad \text{with} \quad EI = E\pi r^3 t \quad \text{and} \quad \kappa = \frac{\varepsilon_{\max}}{r} = \frac{\sigma_{\max}}{Er} \\ &M_y = \sigma_y \cdot \pi r^2 t \qquad \kappa_y = \frac{\varepsilon_y}{r} = \frac{\sigma_y}{Er} \quad \text{with} \quad r = (D-t)/2 \end{aligned} \tag{1}$$

And for the elastic-plastic part [6]:

$$M = M_{\mathrm{p}} \cdot 0{,}5\left(\frac{\theta}{\sin\theta} + \cos\theta\right) = 4r^2 t\sigma_y \cdot 0{,}5\left(\frac{\theta}{\sin\theta} + \cos\theta\right) \;\; ; \;\; \kappa = \frac{\varepsilon}{r} = \frac{\varepsilon_y}{r \cdot \sin\theta} \tag{2}$$

where:

$$\theta = \arcsin(\varepsilon_y / \varepsilon) \quad \text{with} \quad \varepsilon \geq \varepsilon_y \tag{3}$$

Fig. 2 gives the stress distribution in the elastic-plastic part and the bending moment curvature diagram without other influences. The curvature is normalized by dividing it by the following quantity:

$$\kappa_I = \frac{t}{D_m^2} = \frac{t}{(D-t)^2} \tag{4}$$

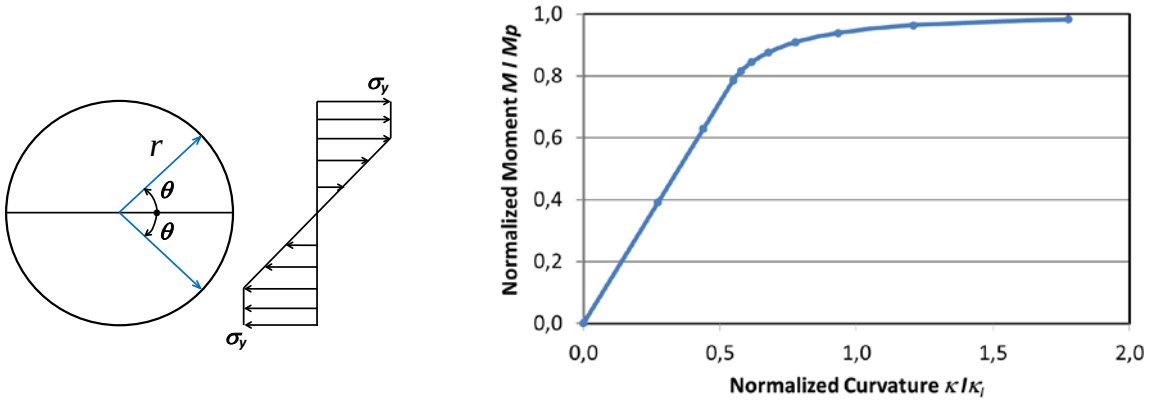

Fig. 2: Stress distribution in bending and bending moment curvature diagram

2.2 Ovalisation

2.2.1 Elastic behaviour

The ovalisation in the elastic part of the bending moment curvature diagram is [6]:

$$a = \frac{r^5}{\rho^2 t^2} = \kappa^2 \frac{r^5}{t^2} \tag{5}$$

This equation can be derived with the model in Fig. 3.

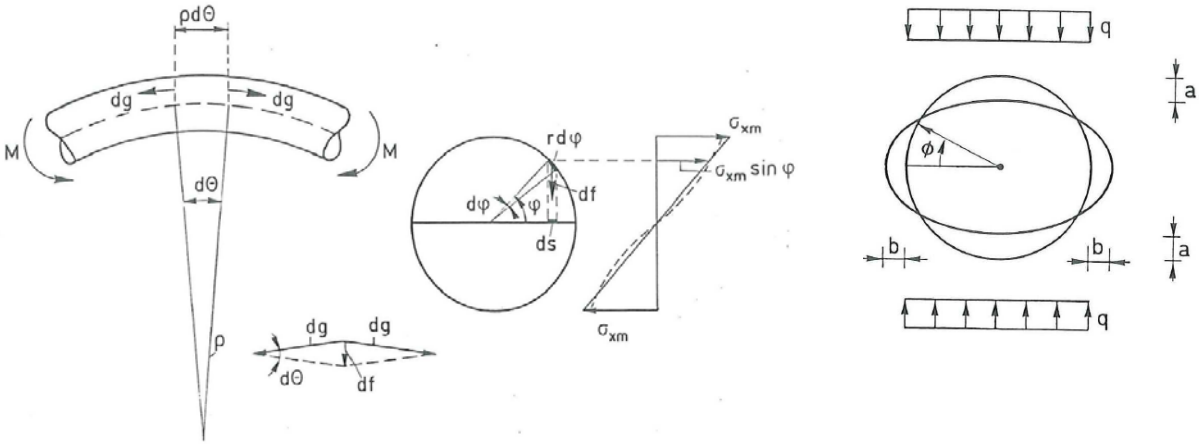

Fig. 3: Ovalisation forces due to linear elastic bending - comparable to a uniform load q [6]

The uniform ovalisation load q and the ovalisation a follow from:

$$q = \frac{df}{\rho \; d\theta \, ds} = \frac{r\,t\,E}{\rho^2} = \kappa^2 r\,t\,E \quad ; \quad a = \frac{q\,r^4}{12EI_{wall}} = \frac{q\,r^4}{12\,E \cdot \frac{1}{12} t^3} = \kappa^2 \frac{r^5}{t^2} \tag{6}$$

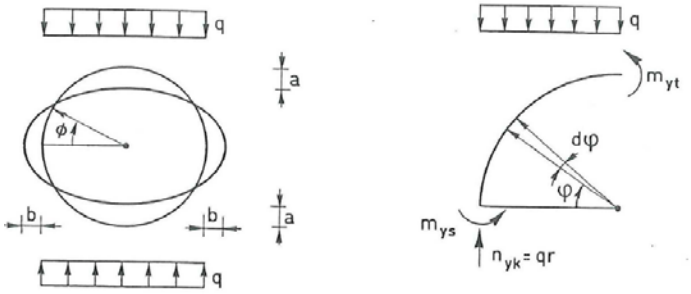

Fig. 4: Ovalisation forces give plate bending moments and plate normal forces

The ovalisation forces cause plate bending moments and plate normal forces in the tube wall (Fig. 4). The model for determining the ovalisation and the plate bending moments enables to take into account and combine these plate bending moments and normal forces with the effect of other loads perpendicular to the tube wall, e.g. soil loads, internal or external pressure and loads from infill sheeting.

2.2.2 Elastic-plastic behaviour

The calculation of the ovalisation in the elastic-plastic part of the bending moment curvature diagram is more complicated. For the full plastic cross section, the normality principle can be applied for the relation between curvature, ovalisation and plate bending moments [6].

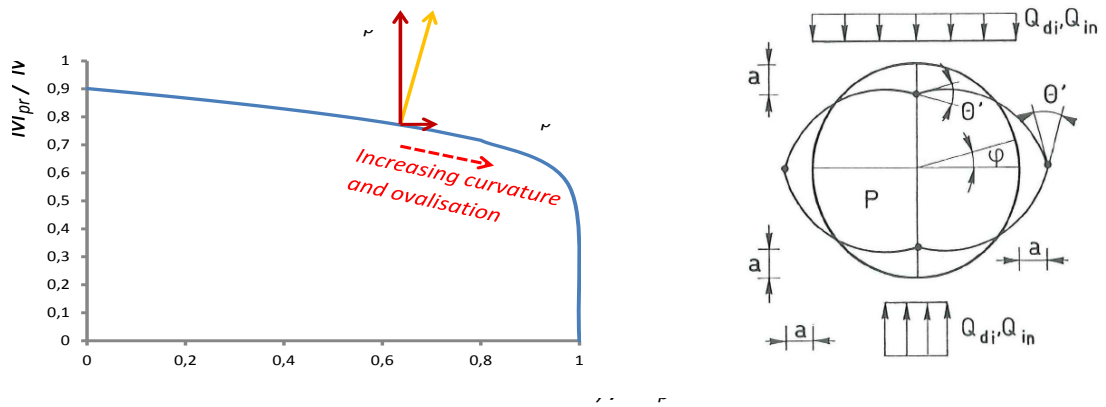

Fig. 5: Yield surface with normality principle and fully plastic cross section

In Fig. 5 the yield surface is given. The plastic moment capacity M_{pr} decreases with increasing values of the plate bending moments. In the right figure, the full plastic cross section with plastic hinges loaded by ovalisation forces and soil loads as in buried pipelines [6] is given. Because the slope of the yield surface is not a constant, a step wise procedure is followed.

$$\delta a = -\frac{r^3}{t}\left(2\psi \cdot \delta \mathrm{K}\right) \quad \text{with} \quad \psi = \frac{dM / M_p}{dm_y / m_y} \tag{7}$$

In this equation, ψ is the slope of the yield surface.

For practical applications an approximate equation is proposed. It is based on the "elastic" model for ovalisation as in Eq. 6. In the elastic part of the bending moment curvature diagram, the ovalisation forces increase due to increasing curvature and increasing axial bending stresses. In the elastic-plastic part, the increase of the ovalisation forces due to bending stresses in axial direction becomes smaller and therefore the ovalisation forces increase slower. For the elastic-plastic part the following equation can be applied for the ovalisation a_p:

$$a_p = \kappa^{1,5} \cdot \kappa_e^{0,5} \cdot \frac{r^5}{t^2} \quad \text{with} \quad \kappa_e = \frac{\varepsilon_y}{r} \tag{8}$$

The area of high plate moments at the sides of the cross section, mainly remains elastic. The plate bending stiffness at the top is governed by the normality principle.

2.3 The effect of ovalisation on the bending moment capacity

Ovalisation gives a reduction in the section modulus and it causes plate bending moments that reduce the tube bending moment capacity. The effect is expressed in next equations:

$$M_{\mathrm{max,oval}} = g \cdot h \cdot M_{\mathrm{p}} \quad \text{with} \quad h = 1 - \frac{2}{3}\frac{a}{r} \tag{9}$$

where g expresses the effect of the plate moments and plate normal forces.

The stresses due to the plate bending moments and plate normal forces are given in Fig. 6. They are optimized to obtain the highest tube bending moment (optimal distribution of stresses according to the theory of plasticity). Plate bending moments in circumferential direction m_y give also plate bending moments in longitudinal direction called m_x (Poisson's ratio ν is assumed as 0,3). Plate normal forces in circumferential direction are n_y and in longitudinal direction n_x. The plate normal forces n_x give the tube bending moment M.

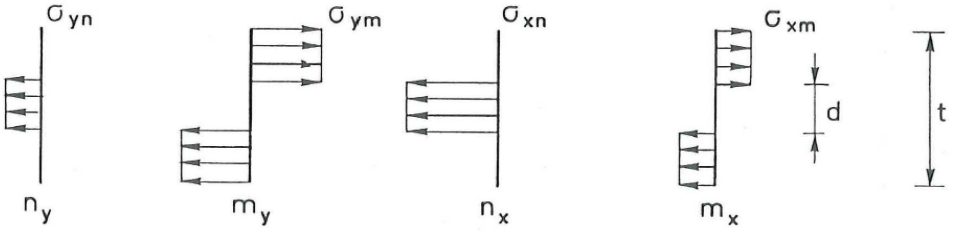

Fig. 6: Plate bending moments and plate normal forces with optimal stress distribution in the tube wall

Once the plate bending moments and plate normal forces in circumferential direction are known, the stresses σ_{xn} and plate normal force n_x can be calculated using the Von Mises yield criterion (Fig. 7). The factor g for tube bending moment capacity can be calculated with:

$$g = \frac{c_1}{6} + \frac{c_2}{3} \tag{10}$$

where

$$c_1 = \sqrt{4 - 3\left(\frac{n_y}{n_p}\right)^2 - 2\sqrt{3}\frac{m_y}{m_p}} \qquad \text{and} \qquad c_2 = \sqrt{4 - 3\left(\frac{n_y}{n_p}\right)^2} \tag{11}$$

with

$$n_y \le n_p = t\, f_y \qquad \text{and} \qquad m_y \le m_p = 0,25\, t^2 f_y \tag{12}$$

The equations for n_y and m_y depend on the type of loading and can be found in [6][3][7]. For pure bending, n_y and m_y are:

$$n_y = 0,20\frac{M_{max}\,\kappa}{r} \qquad \text{and} \qquad m_y = 0,071 \cdot M_{max} \cdot \kappa \tag{13}$$

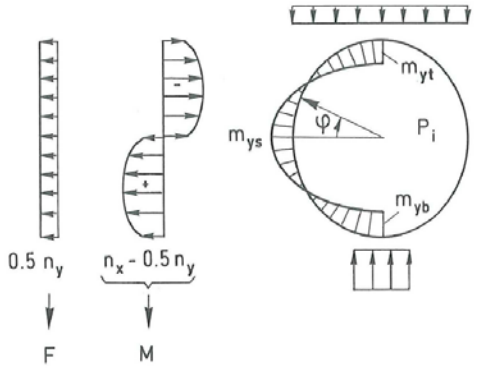

Fig. 7: Plate normal forces in axial direction that give the bending moment in the tube - in the figure also plate normal forces as a result of a normal force in the tube are given

Safe estimates for n_y and m_y can be found by assuming $M_{max} = M_p$ and $\kappa = t/D^2$. The effect of n_y is very small for tubes without internal or external pressure. The effect of ovalisation (reduction of the section modulus) and plate bending moments on the bending moment curvature diagram is depicted in Fig. 8.

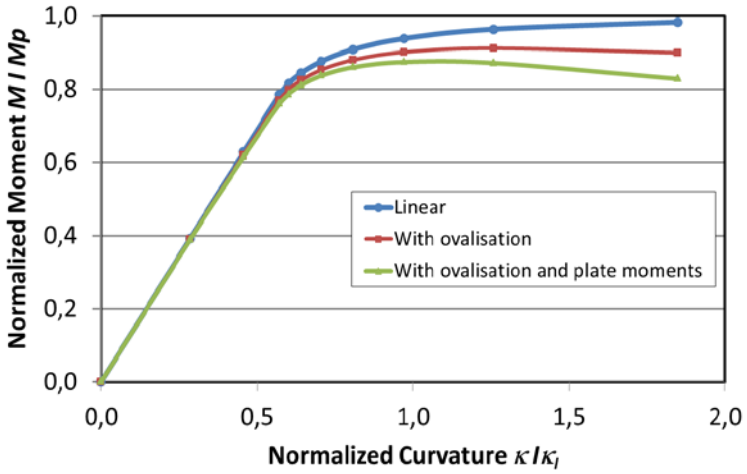

Fig. 8: Effect of ovalisation and plate bending moments on the bending moment curvature diagram

2.4 The effect of residual stresses on the bending moment curvature diagram

Depending on the forming process of the tubes, residual stresses will be present in the tube walls. These residual stresses result in yielding of the tube wall almost from the start of bending. From a bending moment of about $0{,}5M_e$ the effect can be clearly visible. The effect of residual stresses can be taken into account using a modified expression for the curvature.

$$\kappa_{res} = \alpha_{res}\frac{\varepsilon}{r} = \alpha_{res}\frac{\varepsilon_y}{r\cdot\sin\theta} \tag{14}$$

with

$$\begin{aligned} \alpha_{res} &= 1{,}0 && \text{for} \quad M \le 0{,}5M_e \\ \alpha_{res} &= 1{,}0 + \left(\frac{M}{M_p} - \frac{0{,}5M_e}{M_p}\right)^2 && \text{for} \quad M > 0{,}5M_e \end{aligned} \tag{15}$$

The resulting bending moment curvature diagram is given in Fig. 9. It is noted that where the ovalisation is limited, e.g. near endplates, the bending moment capacity will be larger. However, this advantage is only relevant for (very) short tubes and not relevant for tubes in structural applications. Another issue to be taken into account near endplates and connections are the distortions due to welding and uneven introduction of stresses due to variations in stiffness of the supporting structure. In tests it often happens that local buckling occurs near endplates.

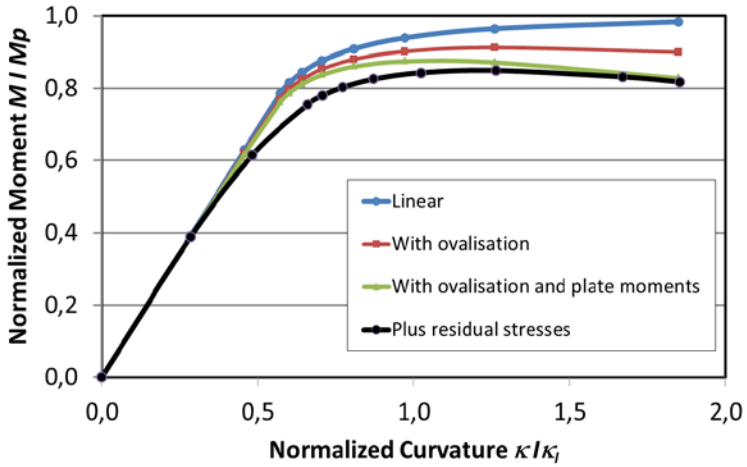

Fig. 9: Effect of ovalisation and plate bending moments and residual stresses on the bending moment curvature diagram

3. Critical curvature for local buckling

3.1 General equations

Starting from the critical strain according to [6][4][3][10], equations have been developed to take into account the various influences that have an effect on the strain at which local buckling occurs. The starting equations are:

$$\varepsilon_{cr} = 0,25\frac{t}{r_o} - 0,0025 \qquad \text{for } \frac{r_o}{t} \le 60$$
$$\varepsilon_{cr} = 0,10\frac{t}{r_o} \qquad \text{for } \frac{r_o}{t} > 60 \tag{16}$$

where ε_{cr} is the critical compressive strain and r_o is the local radius in the compressed part of the cross section as is indicted in Fig. 10.

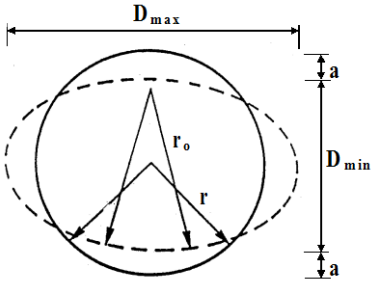

$$r_o = \frac{r}{1-\frac{3a}{r}} \tag{17}$$

$$\kappa_{cr} = \frac{\varepsilon_{cr}}{r_o} \tag{18}$$

Fig. 10: Definition of ovalisation, radius r_o and critical curvature in an ovalised cross section

For pure bending the effect of ovalisation can be neglected because the validation of these equations is done on pure bending tests where ovalisation due to pure bending was included. Therefore, in this case: $r_o = r$. The next equations take into account the other influences.

$$\varepsilon^*_{cr} = \varepsilon_{cr} \cdot \alpha_{geo} \cdot \alpha_{sh} \cdot \alpha_{sand} \quad ; \quad \kappa^*_{cr} = \frac{\varepsilon^*_{cr}}{r_o} \tag{19}$$

where

ε_{cr} is the critical compressive strain in pure bending

α_{geo} is the smallest of the following geometrical imperfections effects:

- α_{un} is the effect of tube surface undulations
- $\alpha_{high-low}$ is the effect of misalignment (high-low) at welds
- α_{dple} is the effect of dimples or dents
- $\alpha_{local-load}$ is the effect of local deformations due to local loads, e.g. waling beams

α_{sh} is the effect of strain hardening

α_{sand} is the effect of sand fill

Below a summary is given of the set of equations to determine these factors.

3.1.1 Surface undulations

For surface undulations the reduction factor for the critical curvature is:

$$\alpha_{un} = a_{un119} - \frac{D/t - 119}{52}(a_{un67} - a_{un119}) \tag{20}$$

with $$\alpha_{un67} = 1,37 - 1,2\left(\frac{\delta_{un}}{2t}\right)^{0,3} \quad \text{and} \quad \alpha_{un119} = 1,15 - 0,5\left(\frac{\delta_{un}}{2t}\right)^{0,3} \tag{21}$$

In these equations is δ_{un} the depth of the undulation (difference between valley and adjacent tops). For undulations δ_{un} equal to 0,04*t*, the factor α_{un} =1,0. This is considered normal quality fabrication. For larger surface undulations, the critical curvature becomes smaller.

δ_{un} /*t*	0,02	0,04	0,08	0,12	0,16	0,20	0,30
α_{un} (*D/t* = 67)	1,07	1,00	0,91	0,86	0,81	0,77	0,69
α_{un} (*D/t* = 93)	1,05	1,00	0,94	0,89	0,86	0,83	0,78
α_{un} (*D/t* = 119)	1,02	1,00	0,96	0,94	0,92	0,90	0,87

The above equations are based on parameter studies in the Combitube project. Canadian research reported by the Center for Reliable Energy Systems (CRES) [12] has resulted in:

$$\alpha_{un-CRES} = 1,84 - 1,6\left(\frac{\delta_{un}}{t}\right)^{0,2} \tag{22}$$

This factor gives about the same reduction for D/t ratios till about 40. It does not depend on the *D/t* ratio. For high *D/t* ratios the CRES reduction factor is much lower than the Combitube result. The field of application in CRES is for D/t between 22 and 104.

3.1.2 Misalignment at girth welds (high-low)

For misalignment at girth welds the following reduction factor can be applied:

$$\text{the smallest of } \alpha_{high-low} = 2,0 - 1,6\left(\frac{\delta_{hl}}{3t}\right)^{0,2} \quad \text{and} \quad \alpha_{hi-lo} = 1,0 \tag{23}$$

Where δ_{hl} is the misalignment at the girth weld as indicated in next table.

δ_{hl} / *t*	0,096	0,15	0,20	0,30	0,40	0,50
$\alpha_{high-low}$	1,0	0,905	0,840	0,742	0,668	0,607

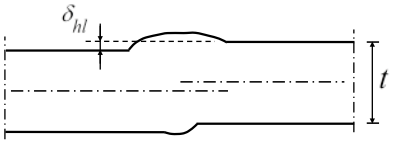

The negative effect of misalignments till δ_{hl} =0,096*t* is assumed to be compensated by the higher yield strength at the weld (overmatched weld metal) and the extra thickness of the tube wall at the weld (the weld cap). The proposed design rule is based on research in [11] and [12]. It was found that for weld high-low misalignments up to 0,50*t*, the effect of the misalignment on the compressive strain capacity is equivalent to a 0,15*t* geometry imperfection (surface undulation) in a plain pipe with zero pressure. Parameter studies in the Combitube project have shown that without the extra thickness of the weld cap and without the overmatched weld strength the effect of misalignments is much larger, as could be expected.

3.1.3 Dimples

For dimples the same reduction factor may be applied as for surface undulations.

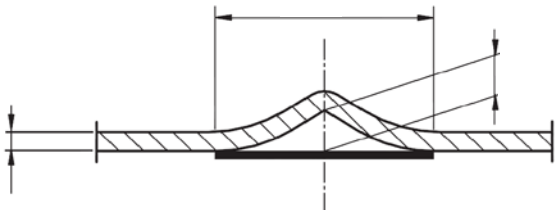

$$\alpha_{dple} = 1,84 - 1,6\left(\frac{\delta_{dple}}{t}\right)^{0,2} \tag{24}$$

The measurement length is according to EN1993-1-6:

$$l_{dpl} = 4\sqrt{rt} \tag{25}$$

3.1.4 Effect of strain hardening

Strain hardening has a positive influence on the local buckling behaviour. The σ_y/σ_t ratio is a measure for the strain hardening.

$$\alpha_{sh} = 1,33 - \frac{0,04}{1-\sigma_y/\sigma_t} \tag{26}$$

σ_y/σ_t ratio	0,82	0,84	0,86	0,88	0,90	0,92	0,94
α_{sh}	1,11	1,08	1,04	1,00	0,93	0,83	0,66
alternative: $\alpha_{sh\text{-}DNV}$	1,11	1,07	1,03	1,00	0,97	0,93	0,91

The factor α_{sh} is based on parameter studies in the Combitube project. The value of α_{sh} is normalised to 1,00 for σ_y/σ_t =0,85. In the DNV rules [13] the following equation is given:

$$\alpha_{strain-hard} = \left(\frac{\sigma_y}{\sigma_u}\right)^{-1,5}, \text{ normalised to } 0,85 \text{ it gives } \quad \alpha_{sh-DNV} = 0,825\left(\frac{\sigma_y}{\sigma_u}\right)^{-1,5} \tag{27}$$

Another formulation is on basis of the strain hardening modulus E_{st}. According to the parameter studies in the Combitube project:

$$\alpha_{sh-combitube} = 1,8 \cdot h^{-0,14} \quad \text{with} \quad h = E / E_{st} \tag{28}$$

h	40	60	80	100	120	140
$\alpha_{sh\text{-}combitube}$	1,07	1,02	0,98	0,95	0,84	0,90

3.1.5 Effect of sand fill

Sand fill has a positive effect on the critical compressive strain, the bending moment capacity and the post buckling behaviour [14][15].

$$\begin{aligned} a_{\text{sand}} &= a_{\text{empty}} \frac{k_{\text{steel}}}{k_{\text{steel}} + k_{\text{sand}}} \\ k_{\text{steel}} &= \frac{12\,EI}{r^4} \left[\frac{\text{N}}{\text{m}^3}\right] \quad with \quad EI = \frac{1}{12} E_{\text{steel}}\, t^3 \qquad k_{\text{sand}} = \frac{E_{\text{sand}}}{r} \left[\frac{\text{N}}{\text{m}^3}\right] \end{aligned} \tag{29}$$

4. Comparison with test results

In Fig. 11 the calculated and measured bending moment curvature diagrams are compared for two of the 14 tested tubes. The column κ_{cr}/κ_I *excl.* in the table on next page gives the critical curvature without the effect of surface undulations and the effect of strain hardening. The column with κ_{cr}/κ_I *incl.* gives the critical curvature including these effects. The lines with K1, K2 and K3 give the measured curvatures along the test tubes [1]. Variations in the bending resistance along the tubes cause variations in the measured curvatures.

Local buckling occurs in the section with the largest curvature. The critical curvature also depends on the measuring length. Test T6D10 had a "coil-connection weld" where the plates from two coils were welded during the spiral-tube production. At that spot large undulations were measured, resulting in a low value of the calculated critical curvature [1] and [7].

Test	D (mm)	t (mm)	D/t	ε_{cr} [19]	κ_{cr}/κ_I ***excl.***	f_y (MPa)	f_u (MPa)	f_y / f_u	α_{sh} [30]	δ_{un} (mm)	α_{un} [24]	κ_{cr}/κ_I ***incl.***
T4D4	1065	9,16	116	0,00184	**0,424**	441	539	0,818	1,11	0,6	0,968	**0,455**
T6D10	1066	16,3	65	0,00526	**0,678**	527	609	0,865	1,03	3,0	0,777	**0,544**

5. Concluding remark

An analytical model is presented that is capable of taking into account many more parameters that have an influence on the bending moment capacity and the deformation capacity than the present equations in the European standards. Addressing these influences enables to much better predict the structural behaviour and lead to less scatter in statistical evaluations of test

data and so enhance economic and safe designs with better balanced safety level.

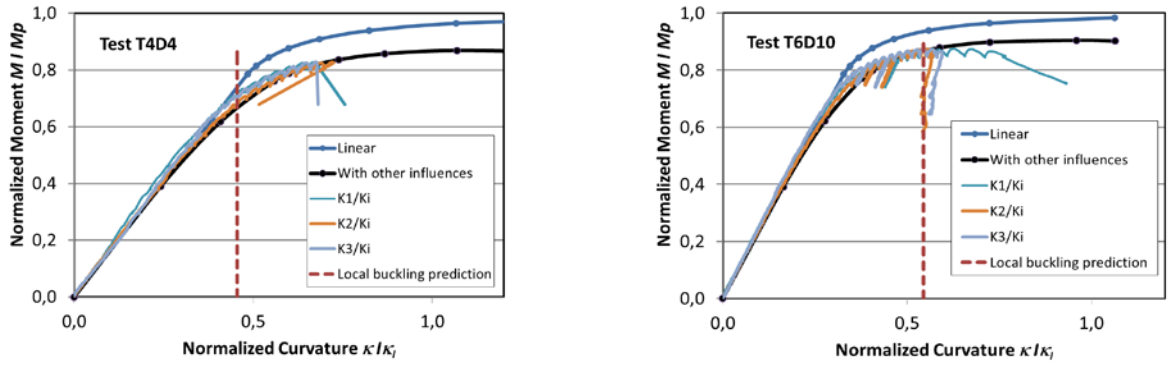

Fig. 11: Test T4D4 and test T6D10 compared with the calculated behaviour, showing good agreement between the tests and the calculations - also showing safe estimates for the local buckling curvature

Acknowledgment

Funding for this work has been provided by the Research Fund for Coal and Steel (RFCS) of the European Commission, project COMBITUBE: "Bending Resistance of Steel Tubes in CombiWalls", Grant Agreement No. RFSR-CT-2011-00034.

References

[1] Van Es SHJ, Gresnigt AM, Vasilikis D, Karamanos SA. "Experimental and Numerical Investigation of the Bending Capacity of Spiral-Welded Steel Tubes", *The International Colloquium on Stability and Ductility of Steel Structures*, Timisoara, Romania, 2016.

[2] EN 1993-1-6 "Eurocode 3: Design of steel structures, Part 1-6: General, Strength and Stability of Shell Structures." *CEN*, 2007.

[3] EN 1993-4-3 "Eurocode 3: Design of Steel Structures, Part 3-4: Pipelines." *CEN*, 2007.

[4] ENV 1993-5 "Eurocode 3: Design of Steel Structures, Part 5: Piling." *CEN*, 1998.

[5] EN 1993-5 "Eurocode 3: Design of Steel Structures, Part 5: Piling." *CEN*, 2007.

[6] Gresnigt AM. "Plastic design of buried steel pipes in settlement areas", *HERON 1986-4*.

[7] European Commission. "Bending resistance of steel tubes in CombiWalls – Final Report", *Research Programme of the Research Fund for Coal and Steel*, Brussels, 2016.

[8] Van Es SHJ, Gresnigt AM, Vasilikis D, Karamanos SA. "Ultimate Bending Capacity of Spiral-Welded Steel Tubes – Part I: Experiments", *Thin Walled Structures*, Vol 102, 286-304, May 2016.

[9] Vasilikis D, Karamanos SA, Van Es SHJ, Gresnigt AM. "Ultimate Bending Capacity of Spiral-Welded Steel Tubes – Part II: Predictions", *Thin Walled Structures*, Vol 102, 305-319, May 2016.

[10] CSA Z662-11. "Oil and Gas Pipeline Systems". *Canadian Standards Association*, 2014.

[11] Nader Yoosef-Ghodsi, Istemi Ozkan, Quishi Chen. "Comparison of compressive strain limit equations". *Paper IPC2014-33182, International Pipeline Conf.*, Calgary, 2014.

[12] Ming Liu, Yong-Yi Wang, Fan Zhang, Kunal Kotian. "Realistic Strain Capacity Models for Pipeline Construction and Maintenance". *Transportation Pipeline and Hazardous Materials Safety Administration Office.* CRES Dublin OH 43017, USA, 2013.

[13] DNV-OS-F101. "Submarine Pipeline Systems". *Det Norske Veritas*, Norway, 2012.

[14] SBRCURnet (2013). "Handbook Quay Walls 2nd Edition." *Centre for Civil Engineering Research and Codes*, Delft, 2013.

[15] Peters DJ, Broos EJ, Gresnigt AM, Van Es SHJ. "Local Buckling Resistance of Sand-filled Spirally Welded Tubes". *Proceedings ISOPE Conference*, Hawaii, 2015.